

## NUMERICAL MODEL TO EVALUATE FIRE RESISTANCE OF RESTRAINED PRESTRESSED CONCRETE BEAMS

**Puneet Kumar<sup>1</sup>, Ph.D. Student**, Department of Civil and Environmental Engineering, Michigan State University, MI. Email: [kumarpu2@msu.edu](mailto:kumarpu2@msu.edu)  
**Venkatesh Kodur<sup>2\*</sup>, University Distinguished Professor**, Department of Civil and Environmental Engineering, Michigan State University, MI (corresponding author).  
Email: [kodur@egr.msu.edu](mailto:kodur@egr.msu.edu)

### ABSTRACT

*Significant fire induced restraint forces can develop in prestressed concrete (PC) flexural members due to high levels of thermal expansion generated in concrete and prestressing strands at elevated temperatures. To trace the development of fire induced restraint forces and its effect on fire resistance of PC beams, a three-dimensional finite element based numerical model is applied in fire resistance evaluation. This numerical model, developed in ANSYS, accounts for critical factors governing fire response of restrained PC beams including joint stiffness, location of restraint, temperature dependent material properties, and cracking and crushing of concrete. The validated model is utilized to undertake a numerical study aimed at quantifying the effect of restraint on fire resistance of PC beams. Based on the results of the numerical study, it can be inferred that magnitude and location of restraint, and trends in evolution of restraint forces can significantly impact fire resistance of PC beams.*

**Keywords:** Prestressed concrete beam, Fire exposure, Finite element model, Restraint force

## INTRODUCTION

Prestressed concrete (PC) beams are integral part of moment frame systems and have to facilitate load transfer under service and extreme conditions. Under fire exposure, PC beam can undergo significant thermal expansion at elevated temperatures; due to high level of thermal expansion in concrete and prestressing strands. Such fire induced expansion of beam is often restrained completely or partially, depending on the beam's connection with framing elements. This restraint to thermal expansion can develop significant additional restraint forces at connections, within beam, and moment frame itself. Also, thermal expansion of beam is highly variable with respect to time and primarily depends on heat transfer between fire and beam, and temperature dependent variation in material properties of constituent materials. This causes continuous variation in magnitude of restraint forces with respect to heating and cooling of beam. Further, at elevated temperatures, concrete and steel lose significant strength and stiffness which introduces more intricacies to the response of restrained PC beams under fire exposure. Therefore, under fire conditions, restraint forces can play a key role in characterizing structural response of PC beams, hence, it is imperative to account for temperature induced restraint forces under fire conditions.

However, there is a lack of experimental and numerical studies aimed at quantifying effect of restraint on fire resistance of PC beams. Most of the building codes follow prescriptive based approach for fire resistance evaluation where a minimum cover to prestressing strands is specified to achieve desired fire resistance [1,2]. This is to keep temperatures in strands below critical temperature (temperature at which strands lose 50% of their strength) and does not capture realistic thermo-mechanical response of PC beams under fire exposure. PCI Manual 124 [3] allows user to design restrained PC beams using a similar criteria for concrete cover to prestressing strands. According to PCI Manual 124 a member is deemed to be restrained if the thermal expansion of member is restrained by framing elements or the gap between member and connecting members is less than 0.25% of the length for normal weight concrete or 0.1% of total length for lightweight and sand-lightweight aggregates. Similarly, other simplified guidelines are provided for structural members to determine whether they should be treated as restrained or not [3]. However, this approach neither evaluates magnitude of restraint forces, nor their impact on local or global response of structure. Further, as PC beams are predominantly designed as flexural load bearing members, they may not withstand high axial restraint forces under fire exposure, and it may lead to partial or complete structural collapse.

Therefore, to overcome these knowledge gaps, a generic three-dimensional (3D) finite element based numerical model is proposed to trace fire response of restrained PC beams under fire exposure. The novelty of proposed model lies in accounting for joint stiffness, location of restraint, and cracking and crushing of concrete. Proposed numerical model is validated using appropriate experimental data from literature by comparing predicted deflection and cross-sectional temperatures against measured values from fire test. Validated numerical model is utilized to undertake a series of case studies on quantifying impact of temperature induced restraint forces on fire resistance of PC beams.

## NUMERICAL MODEL

Fire resistance of restrained PC beams is evaluated using a finite element based numerical model developed in ANSYS [4]. To evaluate fire resistance of PC beam, it is discretized into structural and thermal elements in ANSYS [4], and temperature dependent material properties are assigned to corresponding elements based on Eurocode 2 [5] recommendations. While thermal elements are utilized to simulate heat transfer between fire and beam, and within beam itself; structural elements are utilized to trace corresponding structural response. Also, as output sectional temperatures from thermal analysis serve as input for structural analysis, thermal analysis is carried out first in analysis. For thermal analysis, PC beam is discretized using SOLID70, LINK33, SURF152, and COMBIN39 elements; and they are assigned corresponding temperature dependent thermal properties. SOLID70 is an eight node element capable of simulating conduction and is used to discretize concrete in PC beam. LINK33 is a linear two node element capable of simulating conduction and is used to discretize prestressing strands and steel reinforcement. SURF152 is a four node surface element capable of simulating heat transfer via conduction, convection, and radiation; and is overlaid on surface of PC beam.

This discretized geometry is subjected to fire exposure on relevant surfaces (usually bottom and side faces) and other initial temperature conditions are defined using thermal boundary conditions. The evolution of sectional temperatures is then traced in incremental time steps till the complete duration of fire exposure. At this stage, thermal elements are switched to corresponding structural elements and they are assigned corresponding temperature dependent mechanical properties. SOLID70 is switched to SOLID65, LINK33 is switched to LINK180, SURF152 is switched to SURF154, and COMBIN39 is kept same as it works in structural analysis. SOLID65 is an eight node element utilized to simulate cracking and crushing effects in concrete, LINK180 is a two node element used to simulate prestressing effects in strands and tension and compression in reinforcement. SURF154 is used to apply surface loads on beam, and COMBIN39 is used to simulate beams connection with frame using a 3D non-linear spring. A typical PC beam discretized into several elements is illustrated in Fig. 1.

The stiffness of joint is provided as input to ANSYS as stiffness of COMBIN39 element, and location of connection between COMBIN39 and discretized PC beam represents location of restraint. It should be noted that restraint to thermal expansion of PC beam arises from its connection with other beams and columns at a structural joint (illustrated in Fig. 2). The degree of restraint to thermal expansion of PC beam depends on the combined axial stiffness of the joint. Such combined axial stiffness of joint can be derived by adding axial stiffness contribution from every connecting beam and column at joint and can be computed using Bernoulli's beam element theory. Therefore, restraint from structural joint to thermal expansion of concerned PC beam can be represented using a single non-linear spring (COMBIN 39 element) assigned equivalent axial stiffness of joint under consideration.

Further, to represent typical beam column connections in precast buildings, two generic equations to evaluate combined axial stiffness of structural joint are provided; one for continuous moment resisting connections (illustrated in Fig. 2(a)) and other for simply supported beam column connections (illustrated in Fig. 2(c)). For both equations, it is assumed that four beams meet columns at the structural joint (typical inner joint in a building) as shown in Fig. 2. However, these equations can be further modified by removing beams (contributing stiffness terms in equation) to represent corner or other connection types as well where less than four beams meet at a connection. For all connections, Bernoulli's beam element theory is

utilized to evaluate equivalent axial stiffness of joint. According to this approach, axial stiffness along desired beam (B1) for an interior continuous moment resisting PC beam column joint (illustrated in Fig. 2(a)) can be evaluated as:

$$K_{aBeam\ 1} = \left(\frac{AE}{L}\right)_{Beam\ 1} + \left(\frac{AE}{L}\right)_{Beam\ 2} + \left(\frac{12EI_y}{L^3}\right)_{Beam\ 3} + \left(\frac{12EI_y}{L^3}\right)_{Beam\ 4} + \left(\frac{12EI_z}{L^3}\right)_{Column\ 1} + \left(\frac{12EI_z}{L^3}\right)_{Column\ 2} \dots\dots\dots(1)$$

Whereas, axial stiffness along desired beam (B1) for an interior simply supported beam column connection (illustrated in Fig. 2(c)) can be evaluated as:

$$K_{aBeam\ 1} = \left(\frac{AE}{L}\right)_{Beam\ 1} + \left(\frac{AE}{L}\right)_{Beam\ 2} + \left(\frac{12EI_z}{L^3}\right)_{Column\ 1} + \left(\frac{12EI_z}{L^3}\right)_{Column\ 2} \dots\dots\dots(2)$$

Where,  $K_{aBeam\ 1}$  is total axial stiffness of the connection along Beam 1,  $A$  is area of cross-section,  $E$  is modulus of elasticity,  $L$  is length,  $I_y$  is moment of inertia about y-axis,  $I_z$  is moment of inertia about z-axis; and suffix Beam 1, Beam 2, Beam 3, Beam 4, Column 1, and Column 2 represent that stiffness parameters ( $A$ ,  $E$ ,  $L$ , or  $I$ ) are evaluated for that beam or column. Similarly, axial stiffness along desired beam (B1) for a corner continuous moment resisting PC beam column joint (illustrated in Fig. 2(b)) can be evaluated as:

$$K_{aBeam\ 1} = \left(\frac{AE}{L}\right)_{Beam\ 1} + \left(\frac{12EI_y}{L^3}\right)_{Beam\ 4} + \left(\frac{12EI_z}{L^3}\right)_{Column\ 1} + \left(\frac{12EI_z}{L^3}\right)_{Column\ 2} \dots\dots\dots(3)$$

Whereas, axial stiffness along desired beam (B1) for a corner simply supported beam column connection (illustrated in Fig. 2(d)) can be evaluated as:

$$K_{aBeam\ 1} = \left(\frac{AE}{L}\right)_{Beam\ 1} + \left(\frac{12EI_z}{L^3}\right)_{Column\ 1} + \left(\frac{12EI_z}{L^3}\right)_{Column\ 2} \dots\dots\dots(4)$$

Also, in case of simply supported connections, there is certain gap between beam and column which does not allow restraint forces to develop until thermal expansion of beam surpasses total gap between beam and column. This is simulated by introducing a gap in force displacement curve for COMBIN39 elements, which does not allow spring to be activated until gap is exceeded by thermal expansion of beam. Therefore, in the present study, all beams for which thermal expansion of beam exceeds physical gap provided between beam and connecting members are considered restrained, else, beam is simulated as a non-restrained beam. Final schematic of joint spring and gap connections are also illustrated in Fig. 2.

This stiffness ( $K_{aBeam\ 1}$ ) is assigned to COMBIN39 element to represent 100% axial restraint conditions. However, in real life, thermal expansion is often partially constrained as well; and to represent all such cases joint stiffness can be reduced proportionally to represent reduced degree of restraint effects. In the present study, 50% of restraint conditions are simulated by reducing joint stiffness ( $K_{aBeam\ 1}$ ) by 50%.

The fire response of restrained PC beam is traced in incremental time steps using numerical model discussed above, and it is considered to undergo failure under strength limit state when applied moment on beam under fire conditions surpasses current reduced moment capacity of beam. It is not possible to directly evaluate reduced moment capacity of beam using the results from above finite element based model, as they include nodal deflections and elemental stresses and strains only. Therefore, in the present study, reduced moment capacity ( $M_{nt}$ ) is evaluated at the end of each time step by integrating rational fire design equations proposed by PCI Manual 124 [3] with output nodal temperatures from developed numerical model as:

$$M_{nt} = A_{ps}f_{pst\theta_s} \left(d - \frac{a_t}{2}\right), \tag{5}$$

where,  $A_{ps}$  is area of prestressing steel,  $f_{pst\theta_s}$  is actual stress in prestressing strands at average strand temperature  $\theta_s$  corresponding to time  $t$ ,  $d$  is effective depth of slab, and  $a_t$  is depth of equivalent rectangular stress block at time  $t$ , respectively. In Eq. (2),  $f_{pst\theta_s}$  is evaluated as:

$$f_{pst\theta_s} = f_{put\theta_s} \left( 1 - \frac{0.5 A_{ps} f_{put\theta_s}}{bd f_{ct\theta_c}} \right), \quad (6)$$

where,  $f_{put\theta_s}$  is strength of prestressing strands at average strand temperature  $\theta_s$  corresponding to time  $t$ ,  $b$  is effective width of slab, and  $f_{ct\theta_c}$  is compressive strength of concrete at average temperature in zone of flexural compression ( $\theta_c$ ) corresponding to time  $t$ , respectively. In Eq. (23),  $a_t$  is evaluated as:

$$a_t = \frac{A_{ps} f_{pst\theta_s}}{0.85 f_{ct\theta_c} b}. \quad (7)$$

Once, the reduced moment capacity falls below applied moment under fire conditions, PC beam is considered to undergo strength failure, and time to reach same is considered fire resistance of PC beam.

## MODEL VALIDATION

The above numerical model is validated against fire test data on a full scale restrained concrete beam tested by Dwaikat and Kodur [6]. It should be noted that there is a lack of experimental data on fire resistance of restrained prestressed concrete beams. Therefore, experimental study on fire resistance of restrained concrete beam was selected for model validation. This is since only key difference between restrained reinforced and precast prestressed concrete beam is prestress in strands. Apart from that thermo-mechanical response of the two is identical under fire conditions.

These prestress effects in strands are accounted for in developed finite element model using initial stress condition in strand LINK180 elements, and not using different set of elements. This makes applying prestress effects analogous to applying different loads (initial conditions) in the model. Also, the well-established premise of finite element models is that if discretized geometry can successfully capture the thermo-mechanical physics of the beam, then the same model can be utilized to represent its behavior under different loading scenarios. Since, same finite element model is used to simulate fire response of both reinforced and prestressed concrete restrained beams in the present study, therefore, validating numerical model for restrained reinforced concrete beam makes it applicable for prestressed concrete beams as well.

Predicted sectional temperatures and mid span deflections are compared against measured values to establish validity of the model and to gauge its accuracy. Dimensions of beam measure at 254 x 406 x 3960 mm (10 x 16 x 156 in.), and it constitute calcareous aggregate based concrete with a uniaxial compressive strength of 58.2 MPa (8.44 ksi). Main tension reinforcement of beam constitutes of three 19 mm (0.75 in.) diameter bars, and two 13 mm (0.51 in.) diameter bars were provided as compression reinforcement. For shear reinforcement, 6 mm (0.24 in.) diameter stirrups were provided at a spacing of 150 mm (5.9 in.) over the length of beam. The shear reinforcement in the selected beam for validation was designed so as to attain target flexural capacity in the beam. Yield strength of tension and compression

rebars (deformed rebars) measured at 420 MPa (60.92 ksi), and yield strength of stirrups (plain rebars) measured at 280 MPa (40.61 ksi). More details on cross-sectional dimensions, location of thermocouples, strain gauges, and displacement transducers can be referred to Fig. 3.

This beam was tested under four point loading scheme (illustrated in Fig. 3) with two point loads of 50 kN (11.24 kips) each with severe design fire exposure shown in Fig. 4 for a total of five hours (from ignition to burnout conditions). During fire test, axial deformation of beam was constrained partially using a rigid plate to represent a flexible connection in buildings. Restraint forces were allowed to increase to the maximum restraint capacity of loading frame, and afterwards, a constant restraint to thermal expansion was maintained; and evolution of restraint forces can be referred to Dwaikat and Kodur [6]. During fire test, beam response in terms of sectional temperatures, developed axial restraint force, and midspan deflection was measured throughout fire exposure duration. Beam showed minor spalling, and no failure was observed at the end of fire test.

This beam was analyzed using above discussed numerical model, and a comparison between predicted sectional temperatures and midspan deflections is illustrated in Figs. 4 and 5, respectively. It can be clearly observed from Figs. 4 and 5 that there is a good correlation between predicted and measured sectional temperatures and midspan deflections. Small variations in temperatures and deflections can be attributed to variation in the actual material properties for concrete and steel in fire test and utilized Eurocode 2 recommendations in this study. Therefore, proposed model can be utilized to predict the fire response of restrained PC beams with reasonable accuracy.

## **EFFECT OF RESTRAINT FORCE ON FIRE RESISTANCE**

To fully understand the effect of restraint on fire response of PC beams a total of 10 parametric studies are conducted with focus on key variables as section type, aggregate type, and axial restraint intensity. Details of these studies are provided in Table 1. Following beam nomenclature was used: BXY\_R\_L where X is assigned either number 1 or 3 (1 for section 12RB16-58S and 3 for section 16RB24-148S), Y is assigned either C or S (C for calcareous aggregates and S for siliceous aggregates), R represents restraint intensity and varies from 0 to 100%, and L represents location of restraint relative to depth of beam and is considered to be 0.5 for all beams. Therefore, beam labeled as B3S\_100\_0.5 represents a beam with section 16RB24-148S, siliceous aggregates, and 100% restraint acting at half depth of beam. In total two PC beam sections were selected from PCI Design Handbook as 12RB16-58S (section 1) and 16RB24-148S (section 3) to represent typical beams used in practice. These sections were then paired with other variables under consideration to quantify the effect of restraint on fire resistance of PC beams. All beams were analyzed under ASTM E119 fire exposure [7] for 4 hours [3] with a load level of 50% of room temperature capacity. This gravity load to develop 50% of moment capacity in beam was applied on the top face of beam using an equivalent uniformly distributed load. Also, concrete strength assumed to be at 50 MPa (7.25 ksi) while strand strength was 1860 MPa (270 ksi) for all beams.

The intensity of axial stiffness at a connection was determined using Bernoulli's beam element, as discussed in section 2. A total of two continuous moment resisting joints were considered for axial stiffness calculations with 12RB16-58S and 16RB24-148S beam sections

similar to connection geometry illustrated in Fig. 2(a). For joint 1, connection was formed using four 12RB16-58S beam sections and two 16 x 16 four strand column; whereas, joint 2 was formed using four 16RB24-148S beam sections and two 16 x 16 four strand column. Therefore, using geometry of connection shown in Fig. 2 (a), Beam 1 to Beam 4 in equation (1) are represented by 12RB16-58S beam sections and Column 1 and Column 2 are represented by 16 x 16 four strand columns. Similarly, Beam 1 to Beam 4 in equation (1) are represented by 16RB24-148S beam sections and Column 1 and Column 2 are represented by 16 x 16 four strand columns in joint 2. The geometry and material properties of the beams and columns used in fabrication of joint 1 and 2 are provided in Table 2. The total axial stiffness of joint 1 and 2 was then determined by using equation (1) for sectional and material properties illustrated in Table 2, and individual contribution of every component is illustrated in Table 3.

It can be clearly noted from Table 3 that stiffness contribution from Beam 1 and 2 alone accounts for about 98% of total axial stiffness of joint 1 and 2. This is due to the fact that stiffness contribution from direct compression or tension ( $AE/L$ ) is significantly higher than the stiffness contribution from flexural bending ( $12EI/L^3$ ). Therefore, axial stiffness of a joint is predominantly governed by stiffness contribution from direct compression or tension ( $AE/L$ ). Further, it should be noted that both joints represent generic internal beam column connections in a building where 4 beams are connected to 2 columns. Other joint configurations (external or corner joints) can also be easily formed using the same framework by removing corresponding beams. The joint stiffness evaluated in Table 3 is utilized to represent complete or partial restraint conditions in the model. For complete restraint, a non-linear spring (COMBIN39 element) with identical joint stiffness was attached to the beam end using a rigid plate (to minimize local stress concentrations). For 50% intensity the total axial stiffness of connection was reduced by 50% and same was assigned to spring representing connection to framing elements.

Evolution of restraint forces under fire exposure for different beam sections, joints, and aggregate types is illustrated in Figs. 6 and 7. Restraint forces increase gradually for all cases in the initial heating of PC beam as beam starts to expand thermally at elevated temperatures. Then a consistent decay in the magnitude of restraint forces is observed when degradation in material properties cause rapid increase in deflections. With increase in mid span deflections, magnitude of total thermal expansion is reduced significantly, and continues to reduce as deflections continue to increase. This is the main reason for a consistent decay in restraint forces after attaining their peak values. It can be observed from Figs. 6 and 7 that restraint forces are relatively smaller for calcareous based concrete as compared to siliceous based concrete. This is due to less thermal expansion in calcareous aggregates as compared to siliceous aggregates [5]. Also, it can be observed that peak restraint forces range between 600 kN (134.89 kips) to 800 kN (179.85 kips) for 12RB16-58S beam section, and between 1000 kN (224.8 kips) to 1200 kN (269.77 kips) for 16RB24-148S beam section. Therefore, significant restraint forces get developed in both calcareous and siliceous aggregate based concrete beams even for partial (50%) restraint conditions. Hence, it is important to account for the effect of restraint forces on PC beam and entire structure itself.

The effect of these fire induced restraint forces on mid span deflections of beams is illustrated in Figs. 8 and 9. It can be clearly observed from Figs. 8 and 9 that final mid span deflection for restrained beams is significantly less than as compared to beams with no restraint. To further illustrate this point, a comparison of deflection contours is showed in Fig.

10 for fully restrained and non-restrained beams. This is due to high magnitude of developed restraint forces which apply an additional resisting moment in the beam (arising from secondary P-delta effects) thus minimizing deflections. Similar trends in mid span deflections are observed for all beams studied herein. Also, it should be noted that even for flexible connections (with 50% of original joint stiffness) the deflection response is very close to rigid connections with 100% stiffness. This means that the joint stiffness is so high in magnitude that even 50% of same can significantly impact fire performance of the PC beam.

Further, it can be clearly seen from fire resistance results in Table 4 that restraint increases fire resistance for beams with section 12RB16-58S by 60 minutes, and by 6-12 minutes for beams with section 16RB24-148S. Therefore, it is evident from the results that a much deeper understanding of restraint effects on fire resistance of PC beams is indeed required, and current study at Michigan State university is investigating this aspect.

## CONCLUSIONS

Based on the results presented in the paper, following conclusions can be drawn:

- The proposed finite element model accounts for critical factors governing fire response of restrained PC beams including joint stiffness, location of restraint, temperature dependent material properties, and cracking and crushing of concrete.
- Peak restraint forces range between 600 kN (134.89 kips) to 800 kN (179.85 kips) for 12RB16-58S beam section, and between 1000 kN (224.8 kips) to 1200 kN (269.77 kips) for 16RB24-148S beam section. Therefore, significant fire induced restraint forces can develop in PC beams, which can impact the fire performance of PC beam by introducing additional moments in the beam.
- Restraint forces start to decrease once the material degradation effects become dominant and mid span deflections start to increase rapidly. This is one of the main reasons for decay in magnitude of restraint forces at beam ends.
- Restraint forces have significant impact on the fire resistance of PC beams and increased fire resistance for beams with section 12RB16-58S by 60 minutes, and by 6-12 minutes for beams with section 16RB24-148S. Therefore, it is important to account for restraint effects in the design process.

## ACKNOWLEDGEMENTS

The support of this work by Daniel P. Jenny PCI fellowship and Michigan State University is gratefully acknowledged. Any opinions, findings, conclusions, or recommendations expressed in this paper are those of the authors and do not necessarily reflect the views of these institutions.

## REFERENCES

- [1] PCI Committee (2004) PCI design handbook: precast and prestressed concrete, Sixth Edition. Precast Concrete Institute, Chicago
- [2] ACI Committee 216 (2007) ACI 216.1-07 Code requirements for determining fire resistance of concrete and masonry construction assemblies. American Concrete Institute, Farmington, MI
- [3] PCI Manual 124-18 (2018) Specification for fire resistance of precast/prestressed concrete. Precast Concrete Institute, Chicago
- [4] ANSYS (2015) Mechanical APDL theory reference, version 16.2. ANSYS Inc., Canonsburg
- [5] Eurocode 2 (2004) Design of concrete structures-part 1-2: general rules -structural fire design. European Committee for Standardization, London
- [6] Dwaikat MB, Kodur VKR (2009) Response of Restrained Concrete Beams under Design Fire Exposure. Journal of Structural Engineering 135: 1408-1417
- [7] ASTM E119-16a (2016) Standard Test Methods for Fire Tests of Building Construction Materials. American Society of Testing Materials, West Conshohocken, PA

**Table 1** Details of beams selected to quantify effect of restraint on fire resistance of PC beams. Note: 1 kN/mm = 5.71 kip/in, 1 m = 3.28 ft.

Beam	PCI Section Designation	Aggregate type	Joint Axial Stiffness (kN/mm)	Span (m)	Axial restraint (%)	Load Ratio (%)
B1C_0	12RB16-58S	Calcareous	938.8	8.1	0	50
B1C_100_0.5					100	50
B1S_0		Siliceous			0	50
B1S_50_0.5					50	50
B1S_100_0.5					100	50
B3C_0	16RB24-148S	Calcareous	1657.2	9.1	0	50
B3C_100_0.5					100	50
B3S_0		Siliceous			0	50
B3S_50_0.5					50	50
B3S_100_0.5					100	50

**Table 2** Details of selected beams and columns for joint stiffness analysis. Note: 1 m = 3.28 ft, 1 MPa = 0.145 ksi, 1 Pa = 1.45 x 10<sup>-5</sup>.

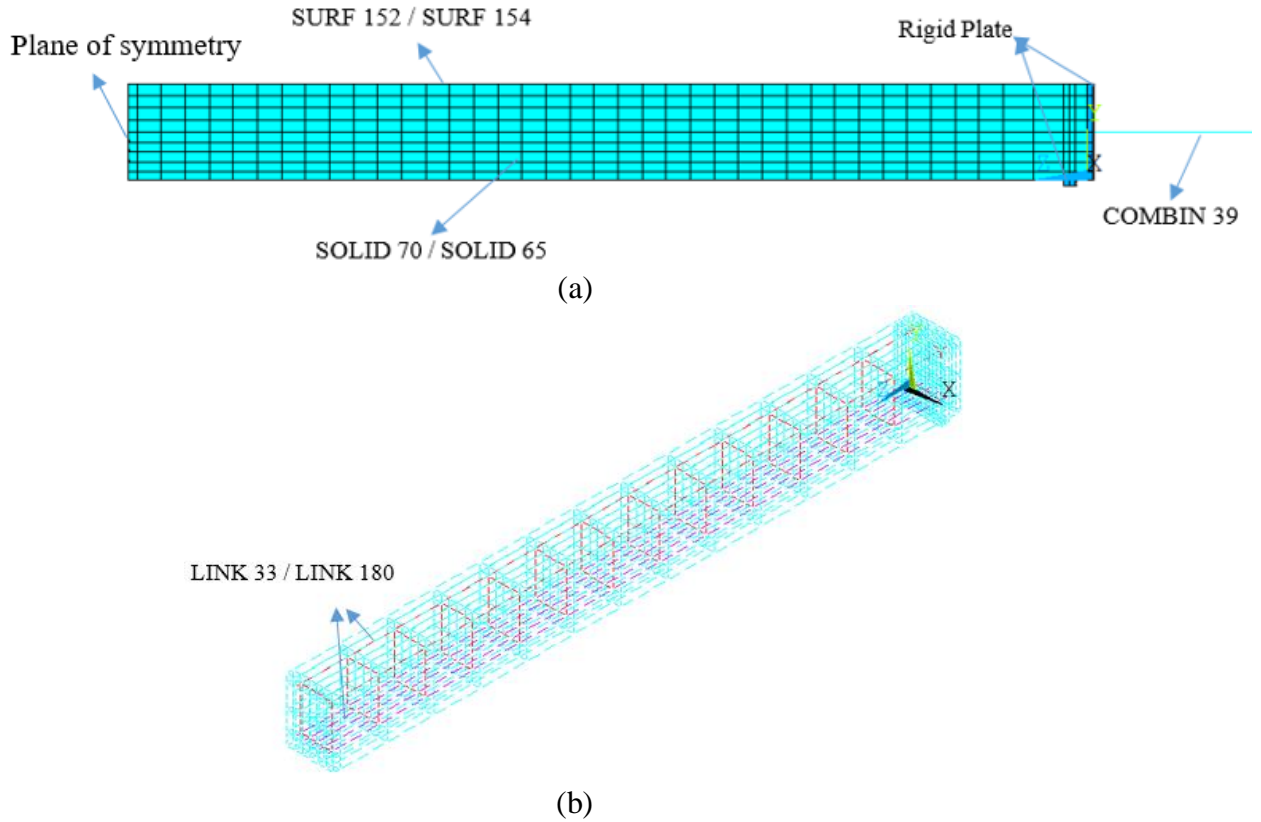
Parameter	12RB16-58S	16RB24-148S	16 x 16-4 strand column
Width (m)	0.305	0.406	0.406
Depth (m)	0.406	0.61	0.406
Length (m)	8.108	9.144	4.5
Concrete Strength (MPa)	50	50	50
Strand Strength (MPa)	1861.5	1861.5	1861.5
Number of strands	Five 12.7 mm diameter strands	Fourteen 12.7 mm diameter strands	Four 12.7 mm diameter strands
Modulus of Steel (Pa)	2E+11	2E+11	2E+11
Modulus of Concrete (Pa)	29069767442	29069767442	29069767442

**Table 3** Axial stiffness calculation for selected joints. Note: 1 kN/mm = 5.71 kip/in.

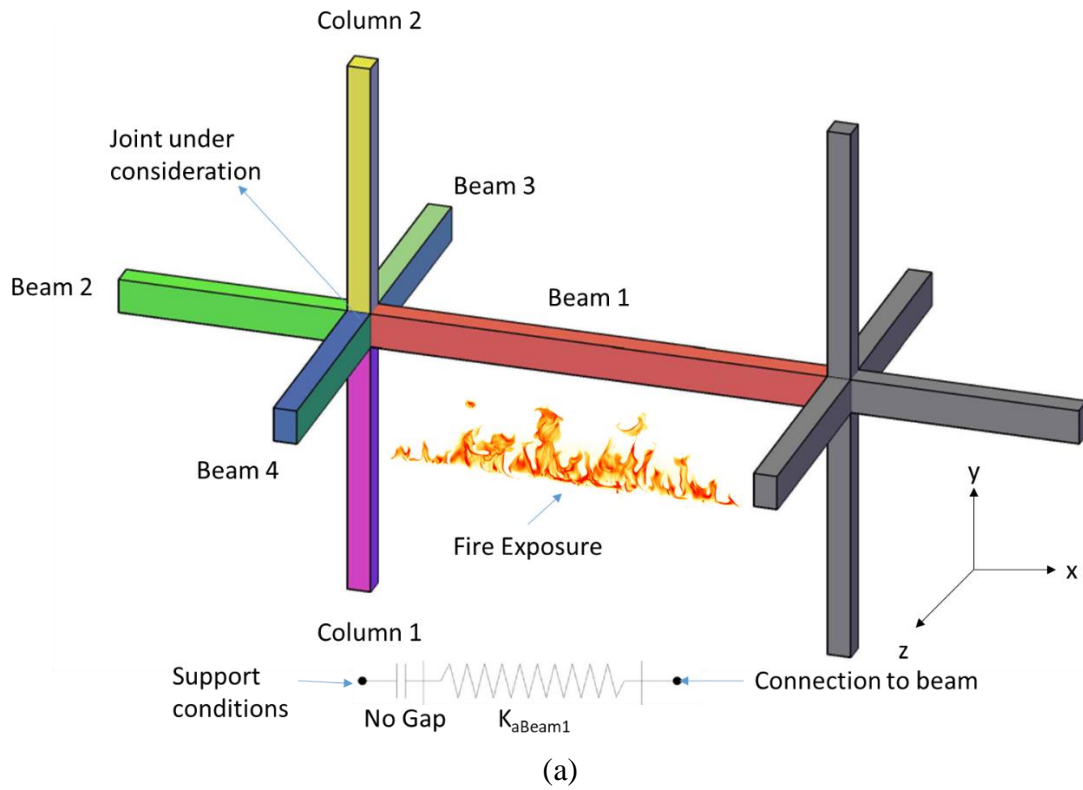
Parameter	Joint 1		Joint 2	
	Section	Stiffness Contribution (kN/mm)	Section	Stiffness Contribution (kN/mm)
Beam 1	12RB16-58S	459.8	16RB24-148S	817.9
Beam 2	12RB16-58S	459.8	16RB24-148S	817.9
Beam 3	12RB16-58S	0.65	16RB24-148S	1.6
Beam 4	12RB16-58S	0.65	16RB24-148S	1.6
Column 1	16 x 16-4 strand column	8.98	16 x 16-4 strand column	8.98
Column 2	16 x 16-4 strand column	8.98	16 x 16-4 strand column	8.98
<b>Total Axial Stiffness (kN/mm)</b>	938.8		1657.2	

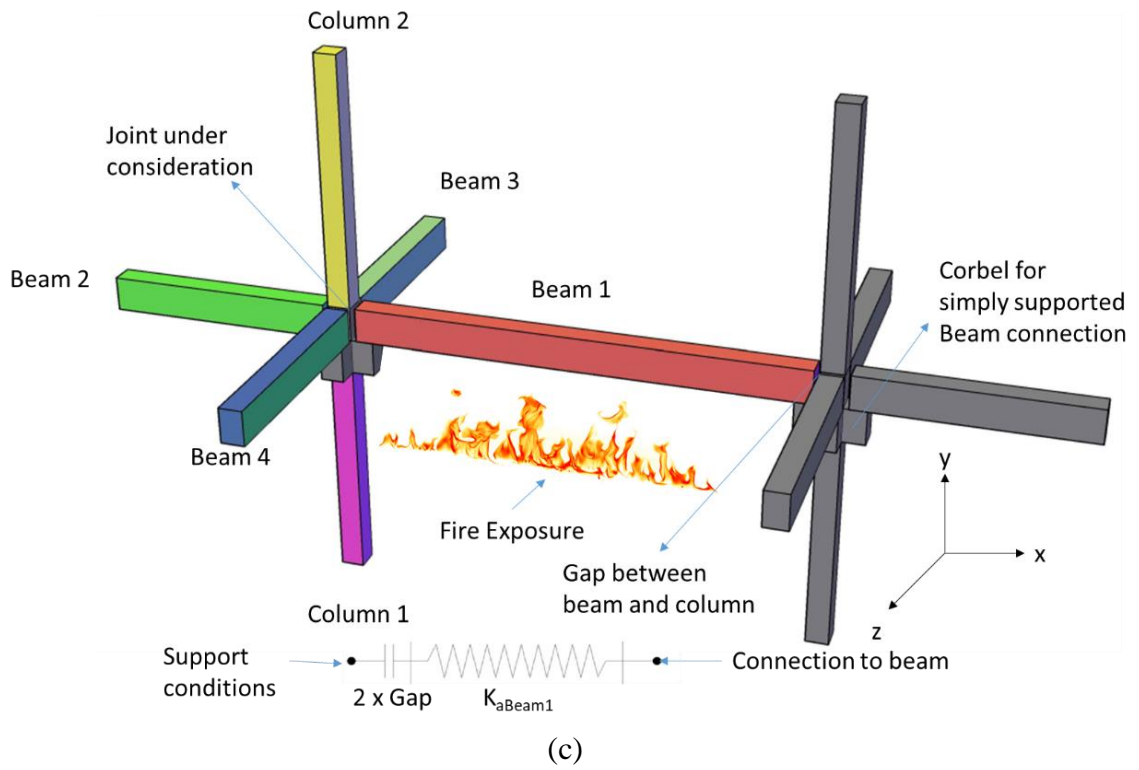
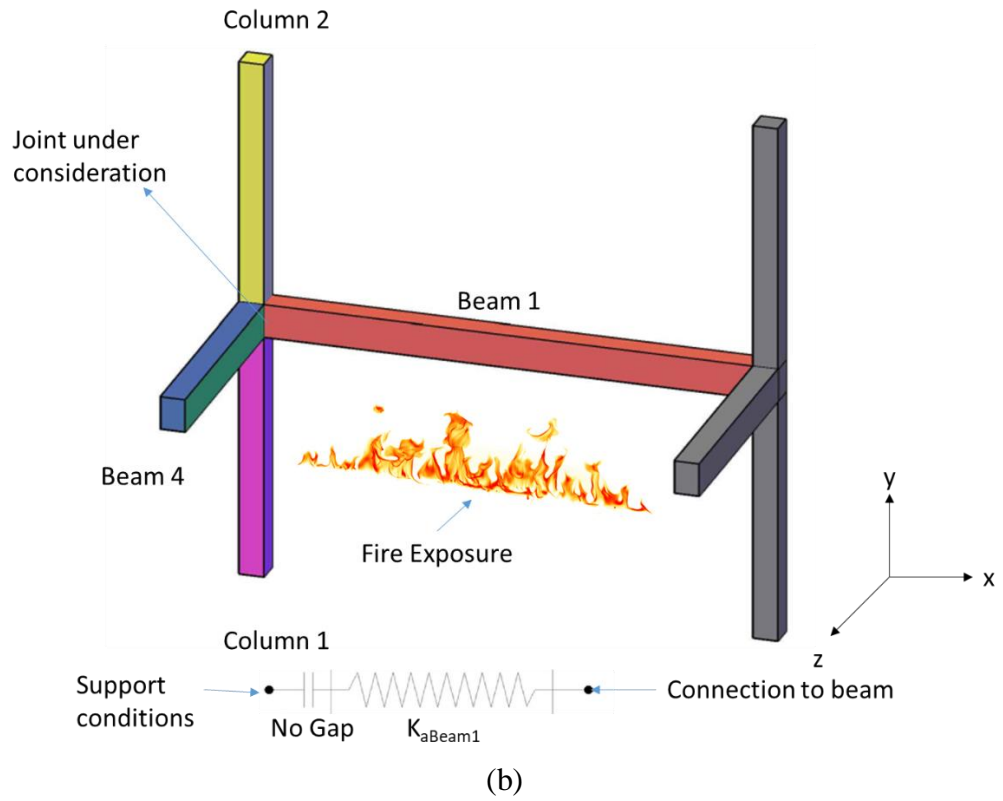
**Table 4** Impact of temperature induced restraint forces on fire resistance

Section Parameters		Fire resistance (min)		
		Restraint (0%)	Restraint (50%)	Restraint (100%)
Calcareous Aggregates	B1C	180	-	240
	B3C	234	-	240
Siliceous Aggregates	B1S	180	240	240
	B3S	228	240	240



**Fig. 1** Discretization of PC beam using various elements for a half symmetric FE model





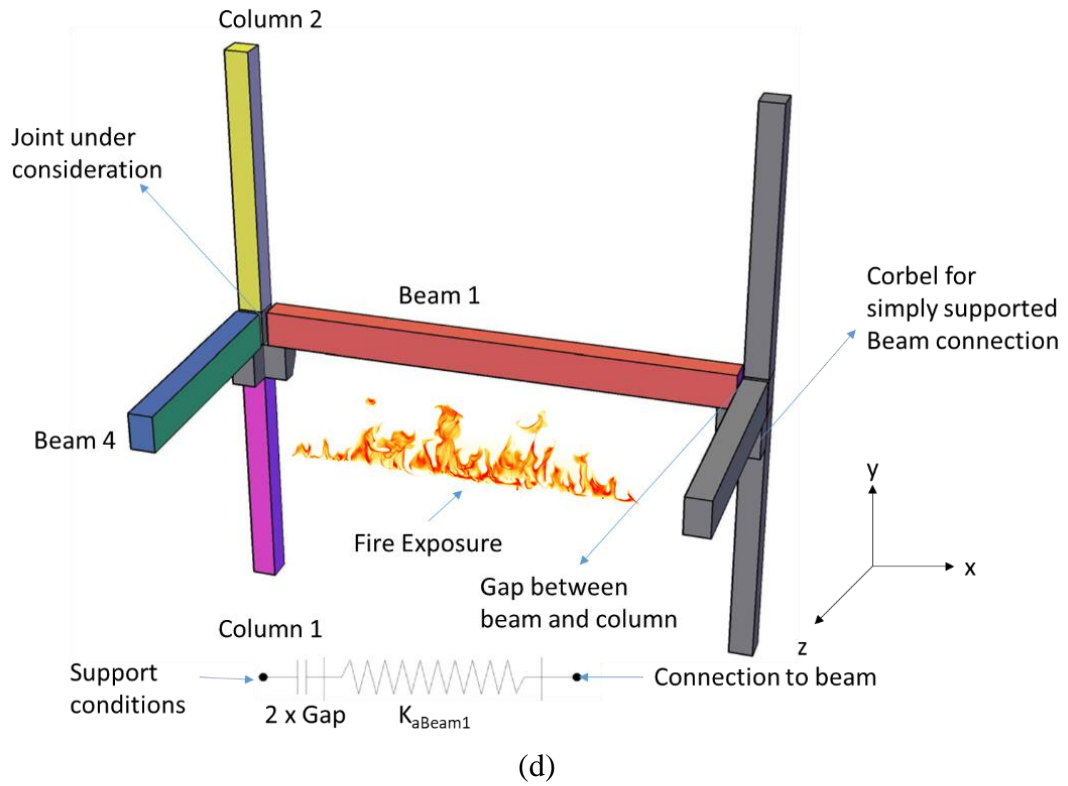


**Fig. 2** (a) Schematic representation of a continuous moment resisting interior beam column connection, (b) moment resisting corner beam column connection, (c) simply supported interior beam column connection, (d) simply supported corner beam column connection

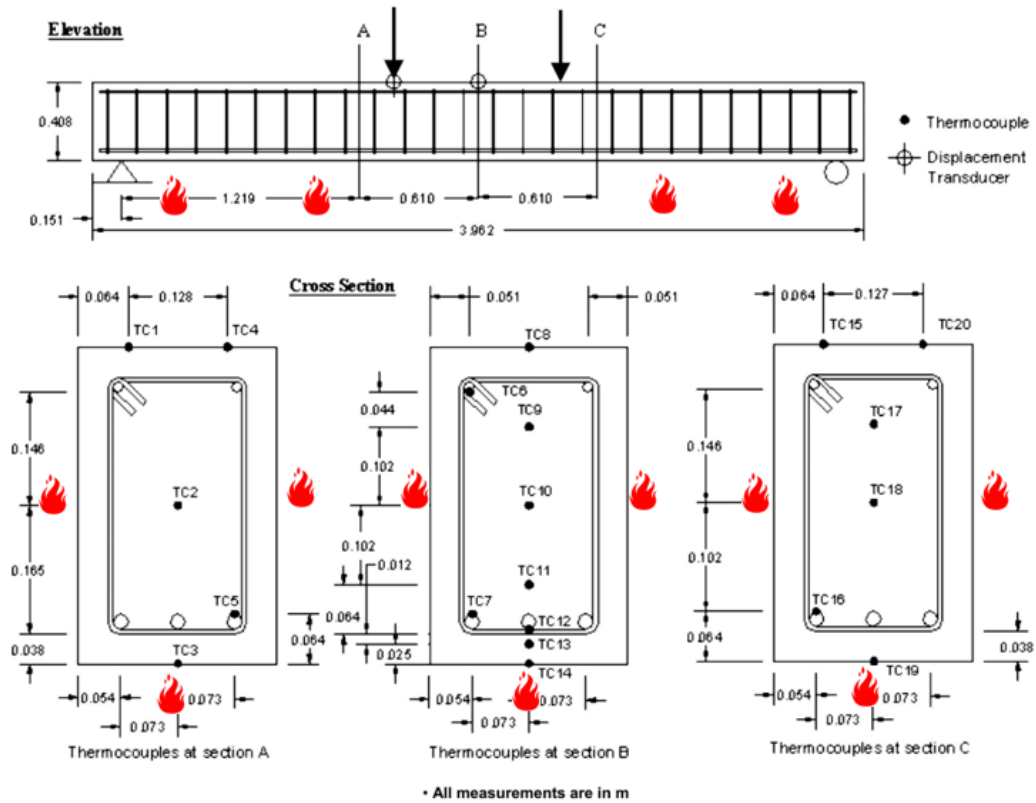


Fig. 3 Cross-section and elevation view of beam selected for validation

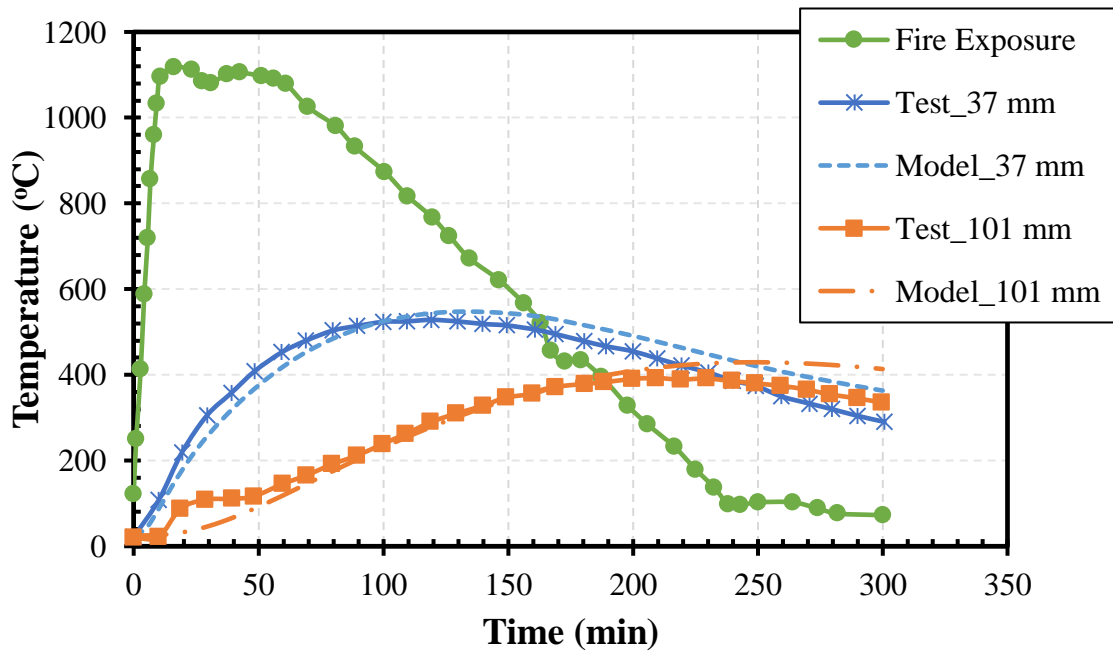
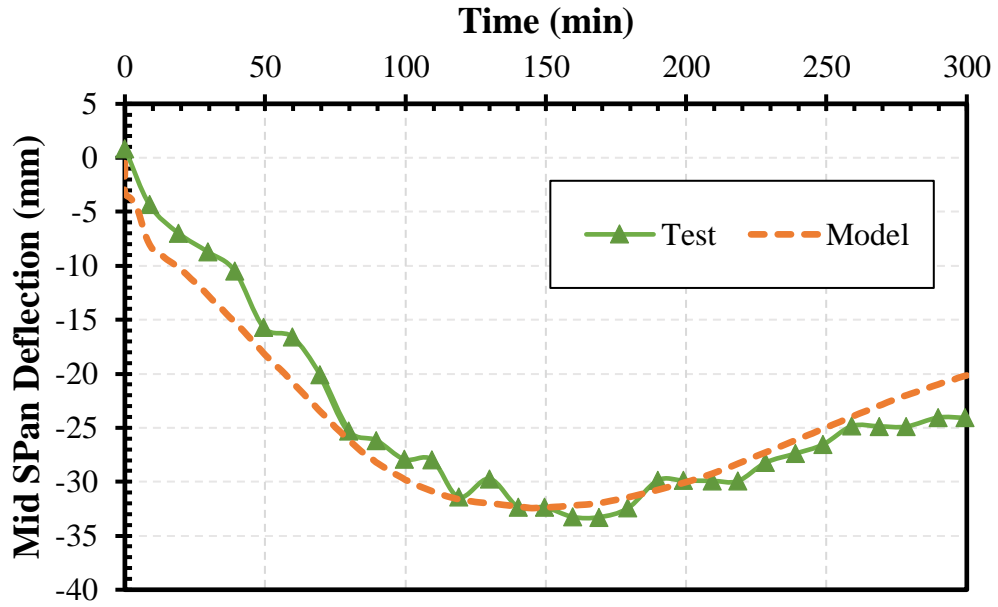
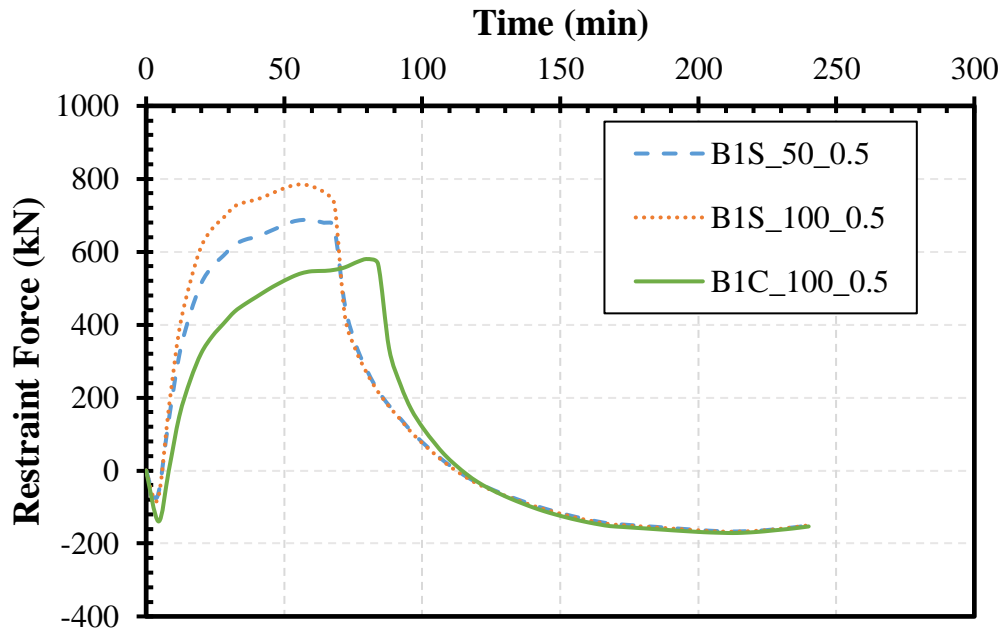


Fig. 4 Comparison between predicted and measured sectional temperatures for beam selected for validation. Note: 1 mm = 0.0394 in.



**Fig. 5** Comparison between predicted and measured midspan deflections for beam selected for validation. Note: 1 mm = 0.0394 in.



**Fig. 6** Evolution of restraint force for joint 1 and 12RB16-58S beam sections. Note: 1 kN = 0.2248 kips.

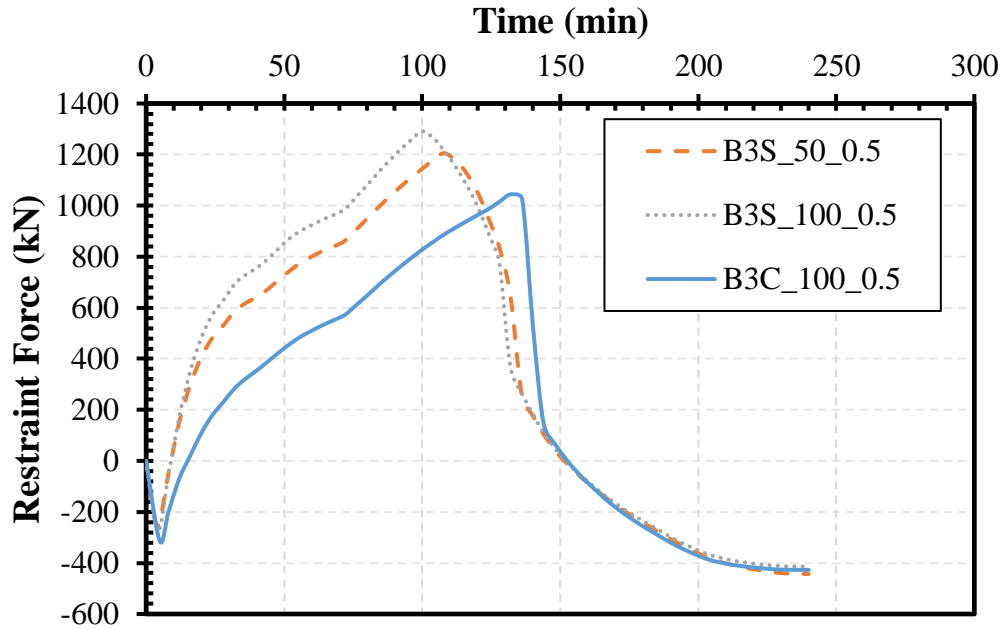


**Fig. 7** Evolution of restraint force for joint 2 and 16RB24-148S beam sections. Note: 1 kN = 0.2248 kips.

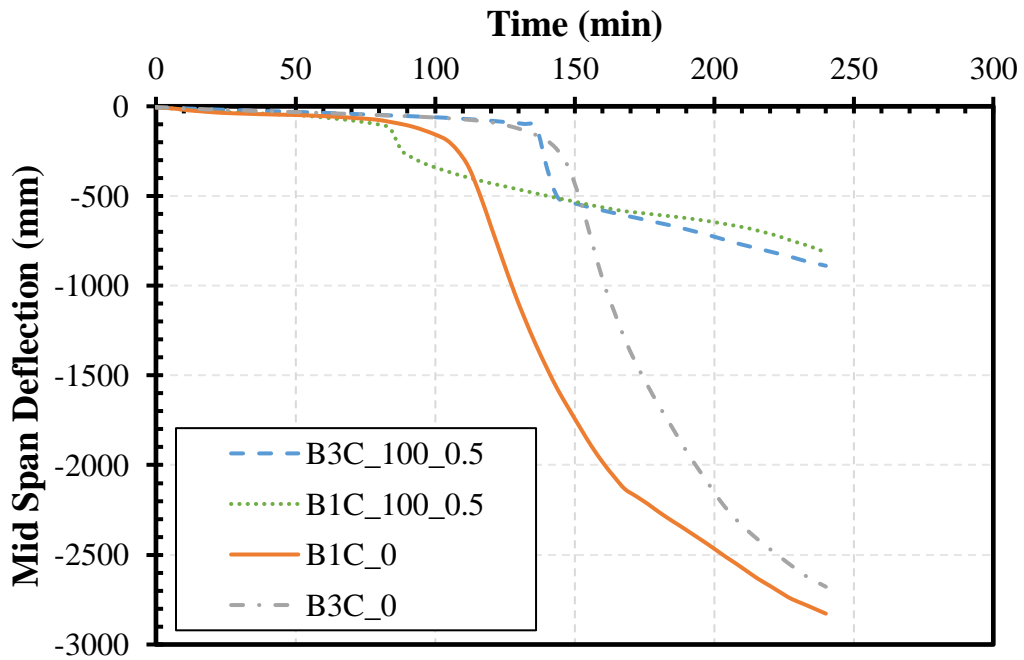


**Fig. 8** Impact of restraint forces on deflection response of calcareous aggregate based restrained PC beams. Note: 1 mm = 0.0394 in.

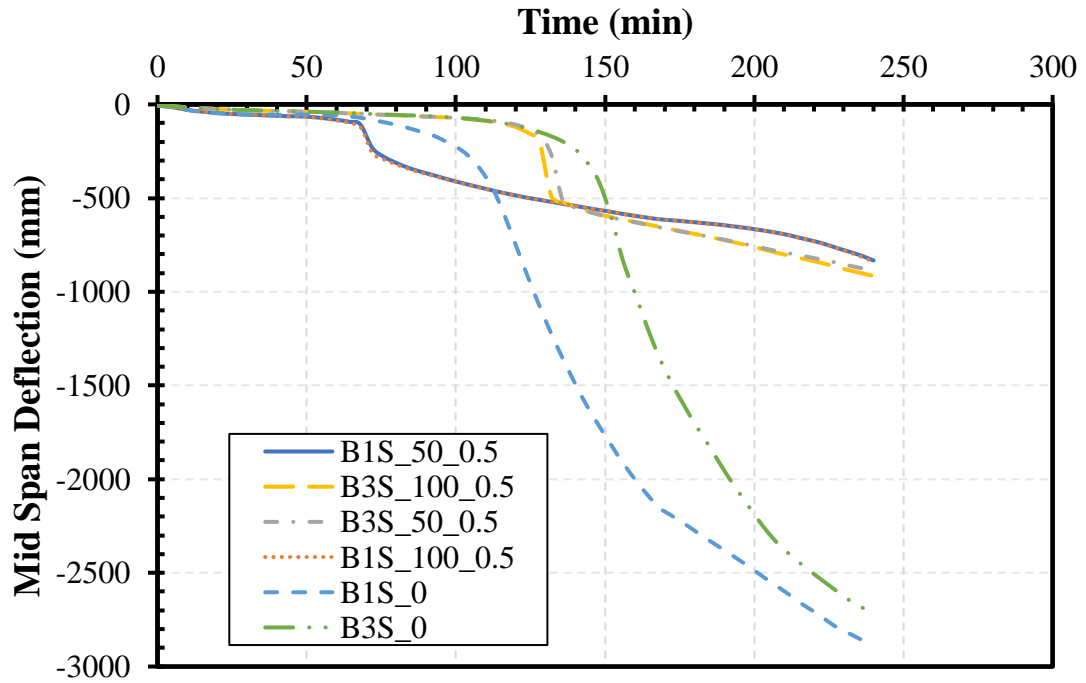
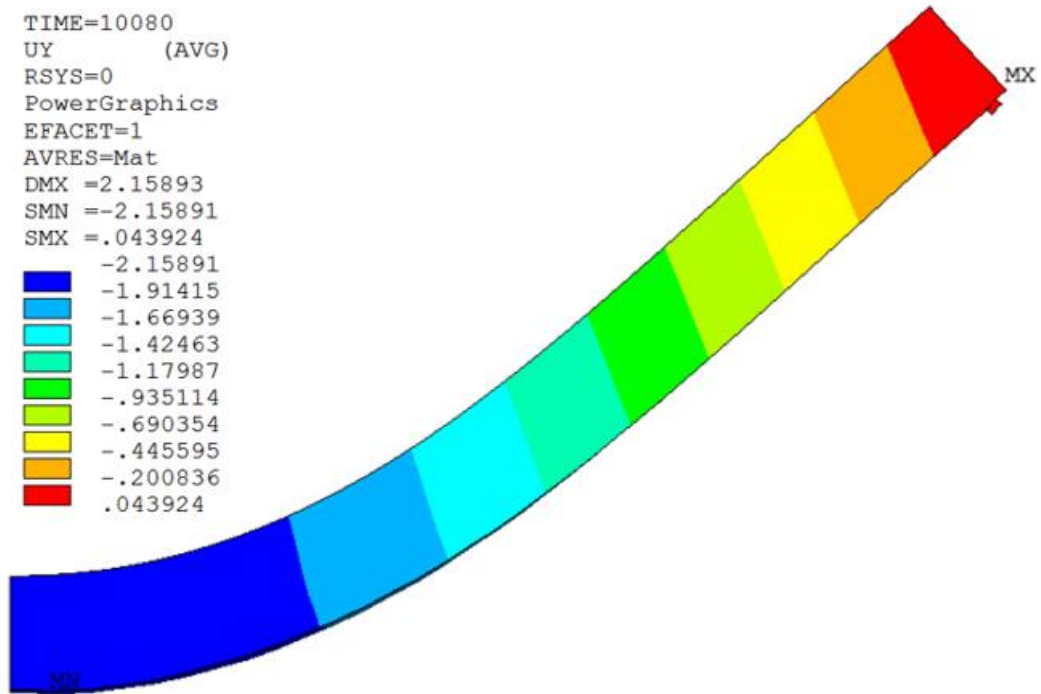
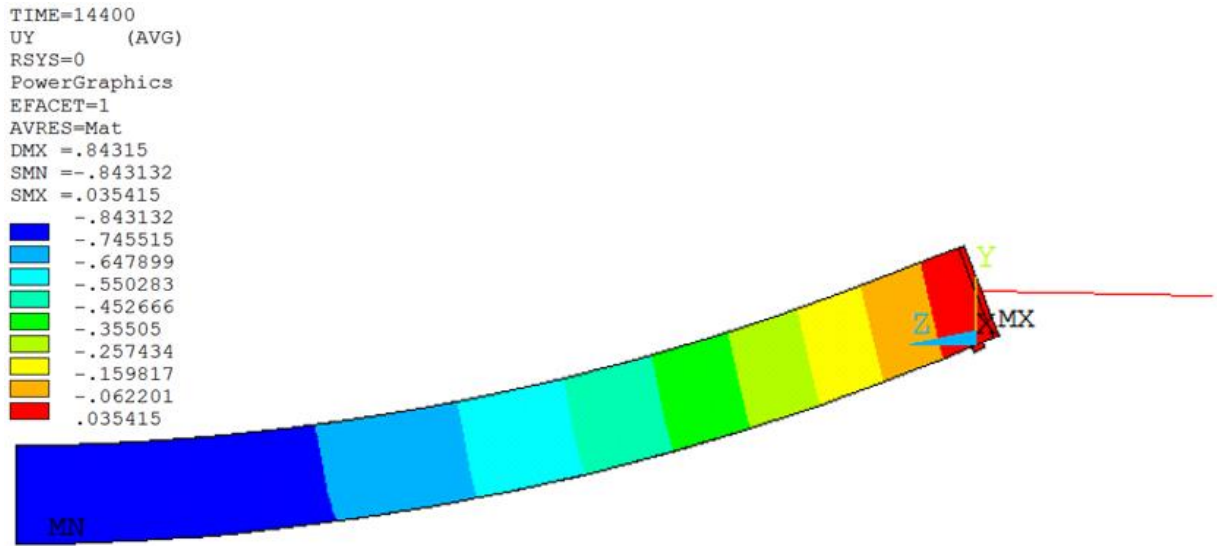


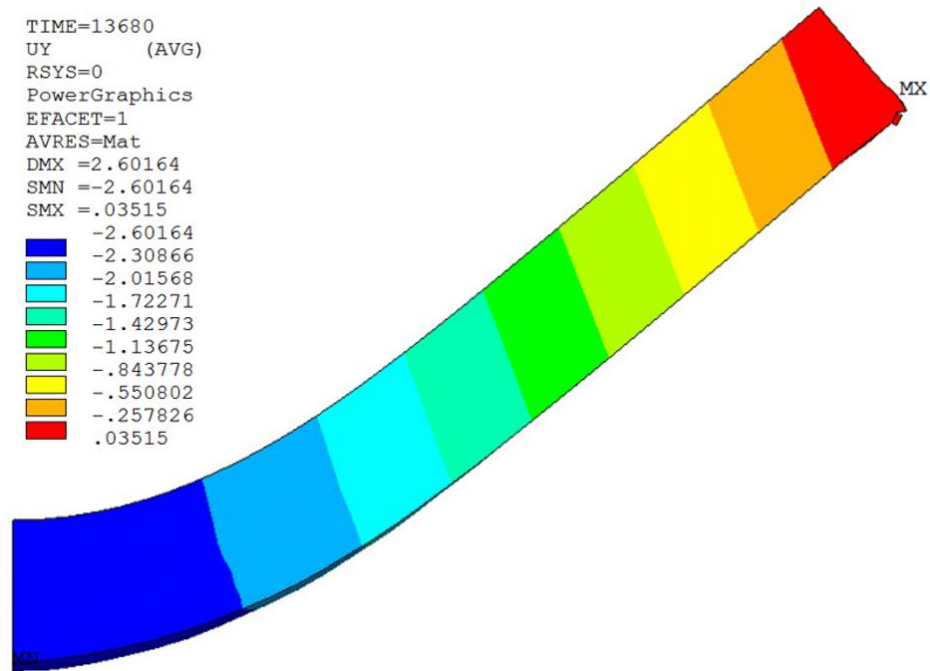
**Fig. 9** Impact of restraint forces on deflection response of siliceous aggregate based restrained PC beams. Note: 1 mm = 0.0394 in.



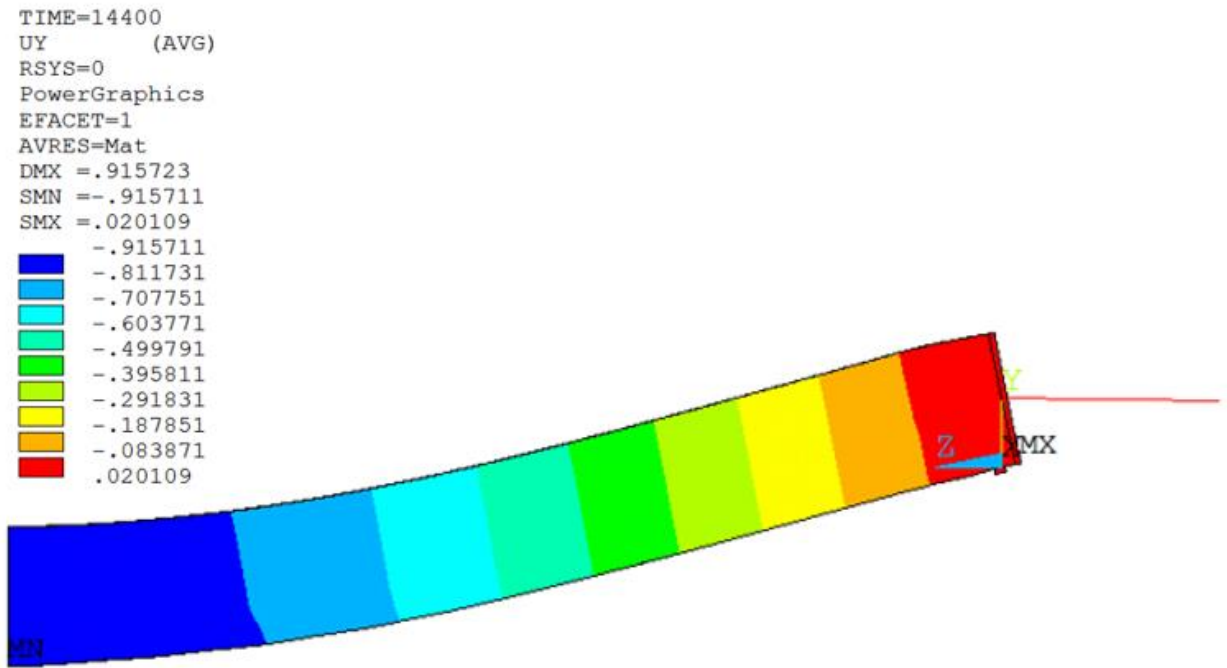
(a) B1S\_0 (Without restraint)



(b) B1S\_100 (With 100% restraint)



(c) B3S\_0 (Without restraint)



(d) B3S\_100 (With 100% restraint)

**Fig. 10** Comparison of deflection contours with and without restraint effects. Note: 1 mm = 0.0394 in.